Accepted Manuscript

Enantiopure (*P*)- and (*M*)-3,14-bis(*o*-hydroxyaryl)tetrahydrobenzo[5]helicenediols and their helicene analogues: Synthesis, amplified circularly polarized luminescence and catalytic activity in asymmetric hetero-Diels–Alder reactions

Lei Fang, Meng Li, Wei-Bin Lin, Chuan-Feng Chen

PII: S0040-4020(18)31269-9

DOI: https://doi.org/10.1016/j.tet.2018.10.047

Reference: TET 29880

To appear in: *Tetrahedron*

Received Date: 8 September 2018

Revised Date: 17 October 2018

Accepted Date: 19 October 2018

Please cite this article as: Fang L, Li M, Lin W-B, Chen C-F, Enantiopure (*P*)- and (*M*)-3,14-bis(*o*-hydroxyaryl)tetrahydrobenzo[5]helicenediols and their helicene analogues: Synthesis, amplified circularly polarized luminescence and catalytic activity in asymmetric hetero-Diels–Alder reactions, *Tetrahedron* (2018), doi: https://doi.org/10.1016/j.tet.2018.10.047.

Graphical Abstract

To create your abstract, type over the instructions in the template box below.
Fonts or abstract dimensions should not be changed or altered.

Enantiopure (*P*)- and (*M*)-3,14-bis(*o*-hydroxyaryl)tetrahydrobenzo[5]helicenediols and their helicene analogues: synthesis, amplified circularly polarized luminescence and catalytic activity in asymmetric hetero-Diels–Alder reactions

Leave this area blank for abstract info.

Lei Fang,[a,b] Meng Li,*[,a] Wei-Bin Lin[a,b] and Chuan-Feng Chen*[,a,b]

[a] *Beijing National Laboratory for Molecular Sciences, CAS Key Laboratory of Molecular Recognition and Function, Institute of Chemistry, Chinese Academy of Sciences, Beijing 100190, China.*
[b] *University of Chinese Academy of Sciences, Beijing 100049, China*

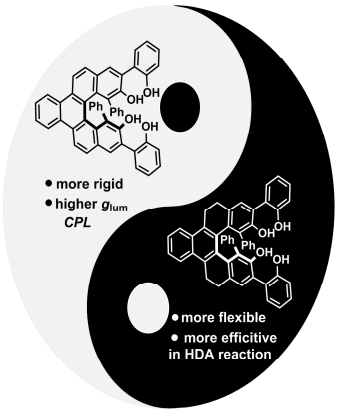

Tetrahedron
journal homepage: www.elsevier.com

Enantiopure (*P*)- and (*M*)-3,14-bis(*o*-hydroxyaryl)tetrahydrobenzo[5]helicenediols and their helicene analogues: synthesis, amplified circularly polarized luminescence and catalytic activity in asymmetric hetero-Diels–Alder reactions

Lei Fang,[a,b] Meng Li,*[,a] Wei-Bin Lin[a,b] and Chuan-Feng Chen*[,a,b]

[a] *Beijing National Laboratory for Molecular Sciences, CAS Key Laboratory of Molecular Recognition and Function, Institute of Chemistry, Chinese Academy of Sciences, Beijing 100190, China.*
[b] *University of Chinese Academy of Sciences, Beijing 100049, China.*

ARTICLE INFO

Article history:
Received
Received in revised form
Accepted
Available online

eywords:
helicenediol
asymmetric catalysis
hetero-Diels–Alder reaction
amplified CPL

ABSTRACT

Three pairs of enantiopure (*P*)- and (*M*)-3,14-bis(*o*-hydroxyaryl)tetrahydrobenzo[5]helicenediols (ArOH-H[5]HOLs), and enantiomers (*P*)- and (*M*)-3,14-bis(*o*-hydroxyphenyl)benzo[5]helicenediols (PhOH-[5]HOLs) were designed and synthesized. It was found that compared with ArOH-H[5]HOLs, PhOH-[5]HOLs not only showed obvious red-shifts in both absorption and emission spectra, but also exhibited more intense CPL with amplified g_{lum}, which might be attributed to the more rigid structure of PhOH-[5]HOLs. However, rigid PhOH-[5]HOLs was less e□ective in the catalytic asymmetric hetero-Diels–Alder (HAD) reactions than those of ArOH-H[5]HOLs with the flexible tetrahydro[5]helicene backbone that could adjust conformation to suit the substrates. Therefore, the helical chirality amplification and chirality transfer could be efficiently achieved by adjusting the rigid and flexible structures of helical molecules, which might provide a useful strategy to optimize the structure of helicence derivatives for their applications in chiroptical materials and asymmetric catalysis.

1. Introduction

Helicences, a kind of π conjugated compounds with helical structure, were composed of ortho-fused polycyclic aromatic rings [1]. Helicenes and their analogues could be not only applied in a broad range of functional material fields as a result of their expanded π conjugated systems and excellent chiral optical properties [2-8], but also used as asymmetric catalysts due to their helical chirality [9,10]. However, convenient synthesis of multifunctional helicenes and their analogues is a challenge [11]. To improve performance, multifunctional helical molecules could be obtained by introducing functional groups to the precursors. Thus, rational design of the structure of helicenes and their analogues to optimize their properties and functions was still an attractive task.

Helicenes and their analogues were good chromophores as well as important small organic molecules with CPL properties due to their helical π conjugated skeleton [12-18]. For CPL organic materials, a key goal is to achieve their high luminescence dissymmetry factor (g_{lum}), which is used to evaluate the level of CPL, $g_{lum} = 2 \times (I_L - I_R)/(I_L + I_R)$, where I_L and I_R are the intensity of the left- and right-handed circularly polarized emissions, respectively [19]. However, the general method to obtain higher g_{lum} was based on the supramolecular assembly of chiral organic molecules [20-24]. The reports about utilizing structural adjustment to increase g_{lum}, especially for the helical molecules, were very limited. Therefore, a deep understanding of the relationship between rigid-flexible molecular structure and g_{lum} was particularly significant for the rational design of CPL organic molecules with high g_{lum}.

Since the pioneered work reported by Reetz et al. in 1997 [25], many helical catalysts have been reported with different functional groups. Compared with helical catalysis with phosphine groups [26-40] and nitrogenous groups [41-48], the research about hydroxyl-functional helical catalysts [49] was relatively lacking. However, other chiral hydroxy-functional catalysts, such as BINOL and VAPOL, exhibited efficient catalytic activity in many asymmetric catalysis reactions [50,51]. We envisaged that helical structure could be a suitable skeleton to construct a chiral environment efficiently around hydroxyl functional groups, which would make the helicenoidal phenolic catalysts be a fascinating study direction.

∗ Corresponding author. fax: +86-10-62554449; e-mail: cchen@iccas.ac.cn; limeng@iccas.ac.cn

To evaluate the relationship between the rigid-flexible structures and the chiroptical properties as well as catalytic activities, the enantiomers with different rigid or flexible helical skeletons were designed (Fig. 1). Inspired by the structure of BINOL, we introduced the hydroxyl groups into the helical skeletons to construct the tetrahydrobenzo[5]helicenediol derivatives which were supposed to achieve better catalytic activity. Moreover, the more rigid benzo[5]helicenediol derivatives with a helicene core were also synthesized to optimize the chiroptical properties. Herein, we report the synthesis of a series of ArOH-H[5]HOLs (*P*)-/(*M*)-**3a-c** with flexible tetrahydro[5]helicene backbone and ArOH-[5]HOLs (*P*)-/(*M*)-**3d** with rigid [5]helicene backbone by a post-functionalization strategy. The photophysical and chiroptical properties of **3a-d** were investigated by UV/Vis, fluorescence, CD, and CPL spectra. It was found that compared with (*P*)-**3a-c**, (*P*)-**3d** with more rigid structure showed not only red-shifts in both absorption and emission spectra, but also more intense CPL with amplified g_{lum}. Conversely, it was also found that ArOH-H[5]HOLs **3a-c** with more flexible hydrogenated [5]helicene backbone showed better catalytic activity than the [5]helicene derivative **3d** in the catalytic asymmetric HDA reactions. These results indicated that the amplified CPL properties and efficient catalytic activity of the helicene derivatives could be achieved by regulating their rigid-flexible structures.

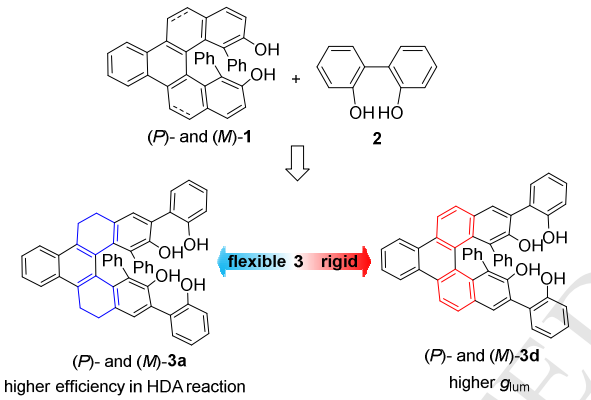

Fig. 1. Design of the enantiomers with different rigid or flexible helical skeletons.

2. Results and discussions

2.1 Synthesis of (P)-3a-d and (M)-3a-d.

The synthetic routes to (*P*)-**3a-c** and (*M*)-**3a-c** are shown in Scheme 1. Starting from the enantiopure Br-H[5]HOL (*P*)-**4** and (*M*)-**4** [3], ArOH-H[5]HOLs (*P*)-**3a-c** and (*M*)-**3a-c** could be conveniently obtained in good yields by Suzuki-Miyaura cross-coupling reaction, respectively. Specific optical rotations of the enantiomeric tetrahydro-benzo[5]helicenes were measured in dichloromethane (DCM), and the enantiomers all showed specific optical rotations of about ±500°. The reaction process does not lead to the racemization of the products and helical tetraols (*P*)- and (*M*)-**3a-c** was identified as enantiomerically pure products by HPLC (ee >99%, Fig. S45-S50, ESI†).

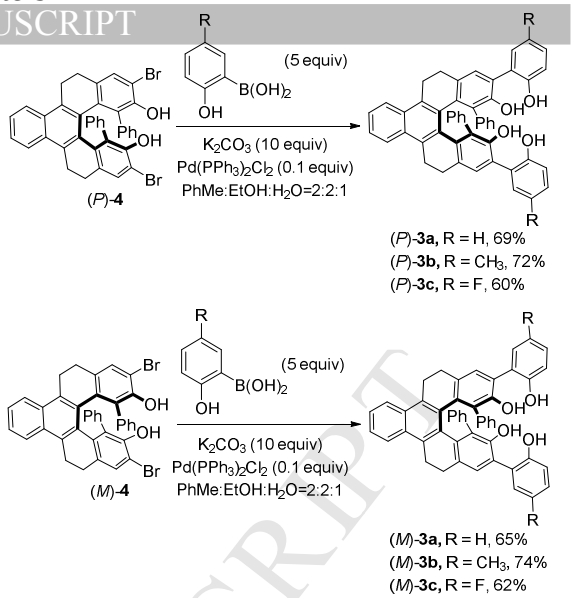

Scheme 1. Synthesis of enantiomers (*P*)-**3a-c** and (*M*)-**3a-c**.

For a comparison, enantiotopic benzo[5]helicene derivative PhOH-[5]HOL was also synthesized. As shown in Scheme 2, (*P*)-**3d** and (*M*)-**3d** could be obtained by the oxidation of MOM-protected tetrahydrobenzo[5]helicene **5** with DDQ, and then followed by their Suzuki-Miyaura cross-coupling reactions with *o*-hydroxyphenylboronic acid, and the deprotected reactions. The specific rotations ($[\alpha]_D^{25}$ in DCM, c = 1.0 mg mL^{-1}) of enantiopure compounds (*P*)-**3d** and (*M*)-**3d** were +1032° and –1056°, respectively, which were larger than those of (*P*)-**3a** and (*M*)-**3a** with a tetrahydro[5]helicene structure.

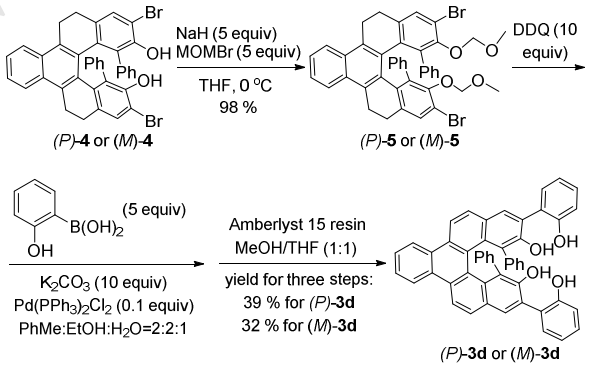

Scheme 2. Synthesis of enantiomers (*P*)-**3d** and (*M*)-**3d**.

2.2 Photophysical and chiroptical properties of (P)-3a-d and (M)-3a-d.

The UV-vis and fluorescence spectra of enantiomers (*P*)-**3a** and (*M*)-**3a** were identical (Fig. S1). Therefore, (*P*)-**3a-d** were then used to investigate their photophysical properties, and the results were summarized in Table 1. It was found that although (*P*)-**3a-c** had different substituted-hydroxyphenyl functional groups at 3,14-positions, no obvious changes of the maximum absorption wavelength for (*P*)-**3a-c** were observed in DCM with the absorption maxima at about 310 nm (Fig. S2 and Table 1). However, compared with tetrahydro[5]helicene analogue (*P*)-**3a**, the enantiotopic helicenoidal tetraols (*P*)-**3d** exhibited obvious red-shift in both absorption and emission spectra. (*P*)-**3d** exhibited the maximum absorption bands at 330 nm with large molar absorptivity (log ε = 4.71), which was 25 nm red-shift compared with that of (*P*)-**3a**. Moreover, (*P*)-**3a-c** all showed a red shift of emission maxima compared with (*P*)-**4**, and exhibited

almost the same emission spectra at about 425 nm with large stokes shifts. Compared with (*P*)-**3a**, the emission spectrum of (*P*)-**3d** exhibited further 31 nm red-shift with stokes shift up to 125 nm (Fig. 2 and Table 1). The fluorescence quantum yields of compounds (*P*)-**3a-c** were all larger than 0.30, with the highest one up to 0.41 of (*P*)-**3c** in DCM upon excitation at the maximum absorption wavelength. For (*P*)-**3d**, its fluorescence quantum yield was 0.19. The partially quenched fluorescence of (*P*)-**3d** might indicate the enhanced π-π stacking interaction and more intense intermolecular electron transfer of the helicene derivatives [52].

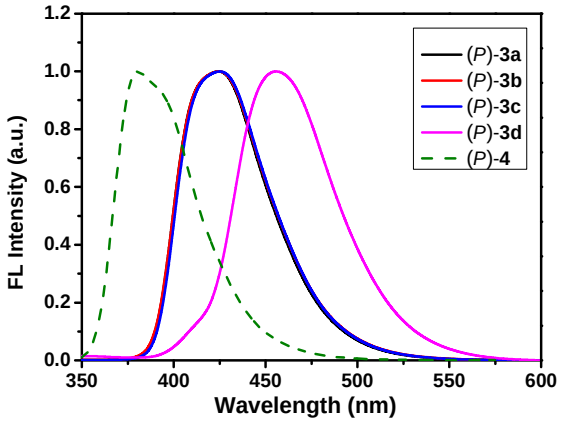

Fig. 2 Fluorescence spectra (excited at corresponding $\lambda_{abs,max}$) of (*P*)-**3a-d** and (*P*)-**4** in DCM (c = 1.0 ×10^{-5} M).

Table 1. Photophysical properties of (*P*)-**3a-d**

Compound[a]	λ_{abs} (nm)[b]	log ε (M^{-1} cm^{-1})	λ_{em} (nm)[c]	Φ_f (%)[d]	$\Delta\lambda_{stokes}$ (nm)[e]
(*P*)-**3a**	305	4.74	424	32.6	119
(*P*)-**3b**	310	4.73	425	41.0	115
(*P*)-**3c**	301	4.74	425	39.1	124
(*P*)-**3d**	330	4.71	455	18.7	125

[a] All spectra were recorded in DCM (c = 1.0×10^{-5} M).
[b] The maximum absorption bands.
[c] Excited at the maxima absorption.
[d] Absolute fluorescence quantum yield.
[e] Stokes shift =λ_{em} − $\lambda_{max,abs}$.

Moreover, it was found that (*P*)-**3a-c** and (*M*)-**3a-c** exhibited mirror images of CD and CPL spectra in DCM. All of the enantiomers showed similar Cotton effects (Fig. 3a), by virtue of the same helical backbones, with strong Cotton effects at about 330 nm, in which the negative signals for (*P*)-**3a-c** and the positive signals for (*M*)-**3a-c** were found. The absorption dissymmetry factors (g_{abs}) were –4.7×10^{-4} to –8.3×10^{-4} for the *P* configuration enantiomers, and +4.9×10^{-4} to +8.7×10^{-4} for the *M* configuration enantiomers, respectively (Table S1, ESI†). Meanwhile, Fig. 3b showed the mirror-imaged CD spectra of (*P*)-**3d** and (*M*)-**3d** in DCM. The g_{abs} value of (*P*)-**3d** and (*M*)-**3d** were –3.28×10^{-4} and +3.57×10^{-4} at 425 nm, respectively, which were similar to their tetrahydro[5]helicene analogues.

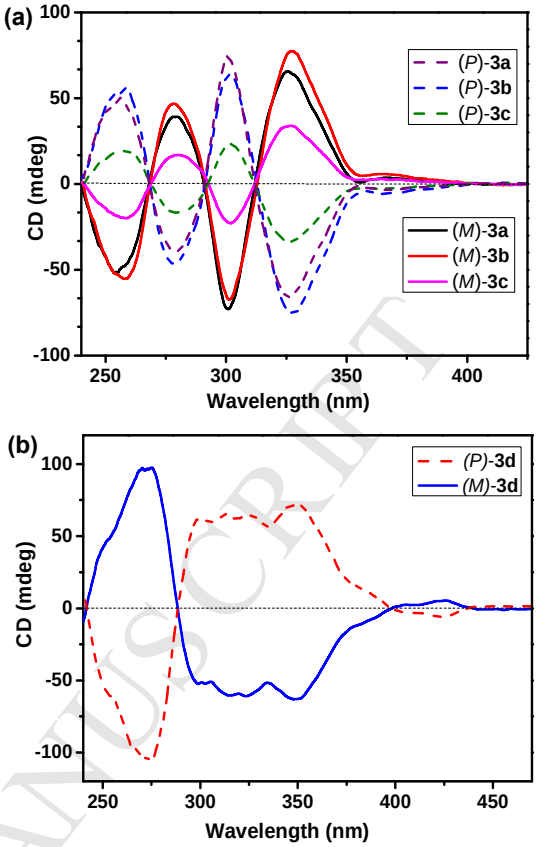

Fig. 3 (a) CD spectra of (*P*)-**3a-c** and (*M*)-**3a-c** in DCM (c = 8.0 ×10^{-5} M); and (b) CD spectra of (*P*)-**3d** and (*M*)-**3d** in DCM (c = 8.0 ×10^{-5} M).

As shown in Fig. 4a, it was further found the enantiomers **3a-c** showed CPL signals, matching with the region of emission spectra. It was noteworthy that the enantiomers exhibited g_{lum} with values of –2.5×10^{-4} to –4.1×10^{-4} for the *P* configuration enantiomers and +2.6×10^{-4} to +4.2×10^{-4} for *M* configuration enantiomers, respectively (Table S2, ESI†). These indicated that the chirality also existed in excited states of enantiomers **3a-c**. Similarly, Fig. 4b showed the mirror-imaged CPL spectra of (*P*)-**3d** and (*M*)-**3d** in DCM. Interestingly, it was found that (*P*)-**3d** and (*M*)-**3d** exhibited CPL emissions with g_{lum} of –4.52×10^{-3} and +4.43×10^{-3} at 455 nm, respectively. The g_{lum} value of which were 20-fold larger than that of PhOH-H[5]HOL (Fig. 4c), which might be attributed to its rigid helical structures that could remained the chirality effectively in the excited states. The results indicated that the CPL amplification can be achieved successfully by the strategy of improving the helical molecular rigidity.

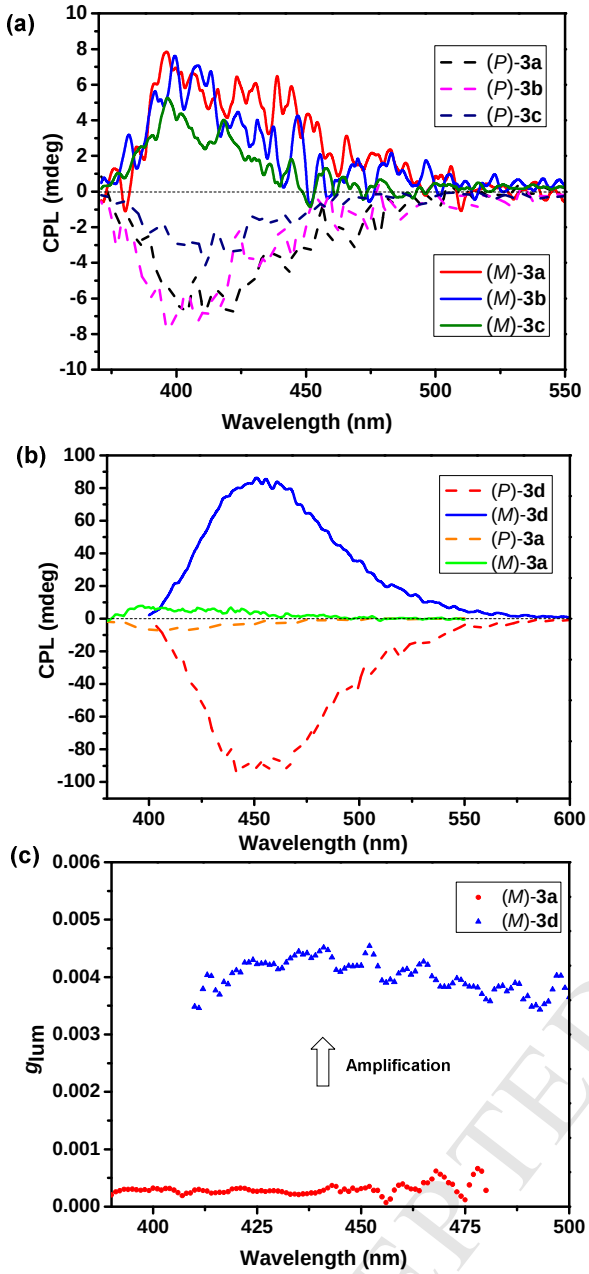

Fig. 4 (a) Mirror image CPL spectra of (*P*)- and (*M*)-**3a-c** in DCM; (b) mirror image CPL spectra of (*P*)- and (*M*)-**3a** and **3d** in DCM; (c) dissymmetry factor g_{lum} versus wavelength of (*M*)-**3a** and (*M*)-**3d** in DCM ($c = 8.0\times10^{-5}$ M).

2.3 Asymmetric catalysis of the helicenoidal tetraols in hetero-Diels–Alder reactions

In view of the successes achieved with Ti/BINOL [53-58], we envisaged helicenoidal phenolic compounds could also be used as asymmetric ligands in HDA reactions. Therefore, we started the catalytic screening by HDA reaction between Danishefsky's diene **6** and benzaldehyde **7a** (Table 2). As a comparison, we first tested the HAD reaction in neat condition with only 10 mol % Br-H[5]HOL (*P*)-**4** as the catalyst, which gave **8a** in 15% yield and no enantioselectivity (Table S3, entry 1). It was also found there was no obvious improvement in yield even when the reaction temperature or solvent was changed (Table S3). By the combination of (*P*)-**4** and Ti(O*i*Pr)$_4$ in toluene, the reaction yield could be increased to 23%, but still no enantioselectivity was shown (Table 2, entry 1). When the post-functionalized PhOH-H[5]HOL (*P*)-**3a** was used as ligand in the presence of Ti(O*i*Pr)$_4$ for the HDA reaction, it was found that product **8a** could be obtained in 68% yield and 23% ee (Table 2, entry 2). We also tested the HDA reaction with the 2,2'-biphenol **2** as ligand, and found that racemic product **8a** was only obtained in 26% yield (Table 2, entry 3). These results indicated that the enantioselectivity of the product with PhOH-H[5]HOL (*P*)-**3a** as ligand was derived from the chirality of helical skeleton.

Table 2. Ligands screening for the enantioselective HDA reaction of Danishefsky's diene **6** and benzaldehyde **7a**[a]

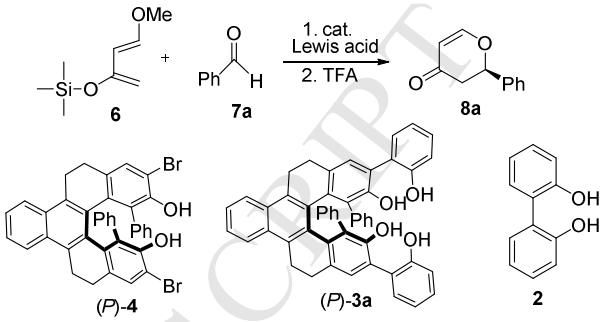

entry	Ligand	Lewis acid	solvent	yield (%)[b]	ee (%)[c]
1	(*P*)-**4**	Ti(O*i*Pr)$_4$	toluene	23	0
2	(*P*)-**3a**	Ti(O*i*Pr)$_4$	toluene	68	23
3	**2**	Ti(O*i*Pr)$_4$	toluene	26	0

[a] All reactions were carried out at 0 °C using 10 mol % of ligand. The ratio of Ti(O*i*Pr)$_4$ and ligand is 2:1. The reaction time was 24 h.
[b] All yields are isolated yields.
[c] Absolute configurations were *R*, which determined in all cases ee was determined by HPLC using a chiral column (Chiracel OD-H).

Besides Ti(O*i*Pr)$_4$, other Lewis acids were also screened for the (*P*)-**3a** catalytic asymmetric HDA reaction of benzaldehyde **7a** with Danishefsky's diene **6**, and the results are shown in Table 3. It was found that butyl magnesium as the Lewis acid decreased the yield and the enantioselectivity (Table 3, entry 2). With trimethylaluminum as the lewis acid, a dramatic improvement in yield (82%) was observed but the enantioselectivity (7%) was poor (Table 3, entry 3). Taking both enantioselectivity and yield into account, Ti(O*i*Pr)$_4$ was chosen as Lewis acid for the catalytic asymmetric HDA reaction.

The effect of the molar ratio of Ti(O*i*Pr)$_4$ to (*P*)-**3a** on the enantioselectivity was examined as well. Stoichiometry ratio of (*P*)-**3a**/Ti was tested from 1:1 to 1:6, the enantioselectivity showed appreciably variation with stoichiometry of Ti(O*i*Pr)$_4$. When the molar ratio of Ti(O*i*Pr)$_4$ to (*P*)-**3a** was 4:1, the best result of 75% yield and 47% ee was achieved (Table 3, entries 1, 4-8). More Ti(O*i*Pr)$_4$ would lead to a decline in enantioselectivity as a result of background reaction.

Different solvents under 1:4 stoichiometry of (*P*)-**3a**/Ti were also screened, which revealed a dramatic solvent effect (Table 3, entries 9-11). It was found toluene was more favorable than other solvents in the Ti(IV)-ArOH-H[5]HOL catalyzed HDA reaction. Reactions with dichloromethane, ether, or dioxane as solvent all gave very low yield as well as poor enantiomeric excess of the product.

We further studied the effect of the amount of catalyst on the HDA reaction. It was found that there was a small decline in the enantioselectivity and yield when the amount of (*P*)-**3a** was increased to 20 mol % or more, which might be due to poor

solubility of the (*P*)-**3a** and excessive amount of Lewis acid causing the background reaction (Table 3, entries 12-13). The temperature profile of the Ti(IV)-ArOH-H[5]HOL catalytic HAD reaction was also performed, and it was found that both yield and enantiomeric excess of the product decreased with increase of the temperature (Table 3, entries 14-15). The optimal temperature of 0 °C could provide the product of the HDA reaction in 79% yield and 53% ee when reaction were pre-activated at 110 °C for 1 h. (Table 3, entry 16).

Table 3. Optimization of the catalytic asymmetric HDA reactions of Danishefsky's diene **6** and benzaldehyde **7a**[a]

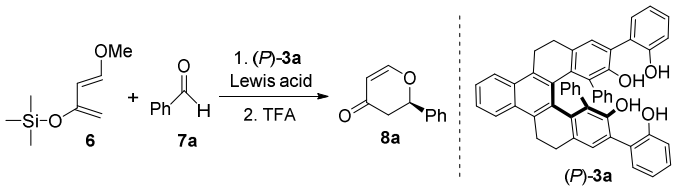

entry	Lewis acid	(*P*)-**3a**: Ti(O*i*Pr)$_4$	solvent	temperature	yield (%)[b]	ee (%)[c]
1	Ti(O*i*Pr)$_4$	1:2	toluene	0 °C	68	23
2	Bu_2Mg	1:2	toluene	0 °C	15	13
3	$AlMe_3$	1:2	toluene	0 °C	82	7
4	Ti(O*i*Pr)$_4$	1:1	toluene	0 °C	42	13
5	Ti(O*i*Pr)$_4$	1:3	toluene	0 °C	73	30
6	Ti(O*i*Pr)$_4$	1:4	toluene	0 °C	75	47
7	Ti(O*i*Pr)$_4$	1:5	toluene	0 °C	72	33
8	Ti(O*i*Pr)$_4$	1:6	toluene	0 °C	70	22
9	Ti(O*i*Pr)$_4$	1:4	DCM	0 °C	15	20
10	Ti(O*i*Pr)$_4$	1:4	dioxane	0 °C	6	<1
11	Ti(O*i*Pr)$_4$	1:4	Et_2O	0 °C	21	14
12[d]	Ti(O*i*Pr)$_4$	1:4	toluene	0 °C	70	43
13[e]	Ti(O*i*Pr)$_4$	1:4	toluene	0 °C	62	38
14	Ti(O*i*Pr)$_4$	1:4	toluene	r.t.	73	25
15	Ti(O*i*Pr)$_4$	1:4	toluene	40 °C	68	27
16[f]	Ti(O*i*Pr)$_4$	1:4	toluene	0 °C	79	53

[a] All reactions were carried out at 0 °C. The reaction time was 24 h.
[b] All yields are isolated yields.
[c] Absolute configurations were *R*, which determined in all cases ee was determined by HPLC using a chiral column (Chiracel OD-H).
[d] The amount of ligand (*P*)-**3a** was 20 mol %.
[e] The amount of ligand (*P*)-**3a** was 30 mol %.
[f] 1:4 stoichiometry of (*P*)-**3a**/Ti(O*i*Pr)$_4$ with 4Å molecular sieves in toluene solution were pre-activated at 110 °C for 1 h.

Under the optimal conditions, (*P*)-**3b-d** were also examined as the ligands for the catalytic asymmetric HDA reactions of benzaldehyde and Danishefsky's diene. Compared with (*P*)-**3a**, Ti(IV) complexes prepared from (*P*)-**3b** and (*P*)-**3c** with a tetrahydro[5]helicene core structure provided the product with similar yields and enantioselectivities (Table 4, entries 2-3). For (*P*)-**3d** with rigid [5]helicene skeleton, although it could also display enantiocontrol in the HDA reaction, lower yield and enantioselectivity than those of (*P*)-**3a-c** were obtained (Table 4, entry 4). Enhanced enantioselective control and reaction rate in ArOH-H[5]HOL-catalyzed HDA reaction might be attributed to their flexible backbone which could adjust the conformation of the helical ligands to adapt to the substrate structures.

After testing the applicability of the Ti(IV)-ArOH-H[5]HOL catalytic asymmetric HDA reactions, we further paid our attention to studying the scope of the reactions by utilizing various functionalized aldehydes. The results indicated the electronic effect of the aldehydes on the enantioselectivity was obvious. It was found the electron-donating substituent showed a positive effect on the enantioselectivity, while the electron-withdrawing substituent had a negative influence for both of meta- and para-substituted benzaldehydes. Under the optimal conditions, *p*-methoxybenzaldehyde afforded product **8b** in 62% yield and 43% ee, while *p*-nitrobenzaldehyde gave product **8f** in 44% yield and significantly low enantioselectivity (11% ee). Similarly, *m*-methyl substituted benzaldehyde (**8g**, 58% ee) gave distinctly higher enantioselectivity than that of *m*-nitrobenzaldehyde (**8i**, 19% ee). These results are agreed with the previously reports of the Ti(IV)-H_8-BINOL catalyzed HDA reactions.[57] In the cases of heteroaromatic aldehydes, the obvious electronic effect was also observed. For electron-rich 2-furaldehyde, product **8j** was obtained in a modest yield and enantioselectivity, whereas electron-withdrawing 3-pyridine-carboxaldehyde only led to a low enantioselectivity (**8k**, 14% ee).

For aliphatic aldehydes, cyclohexylcarboxaldehyde and *n*-nonyl aldehyde, very poor enantioselectivities of the products were obtained.

Table 4. HDA reactions of Danishefsky's diene **6** and benzaldehyde **7a** catalyzed by Ti(IV)-(*P*)-**3a-d**[a]

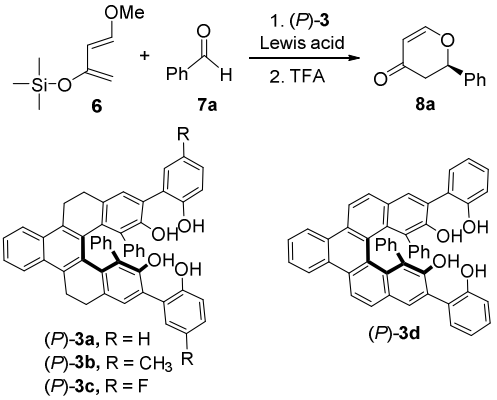

entry	ligand	yield (%)[b]	ee (%)[c]
1	(*P*)-**3a**	79	53
2	(*P*)-**3b**	72	47
3	(*P*)-**3c**	76	53
4	(*P*)-**3d**	60	37

[a] 1:4 stoichiometry of (*P*)-**3**/Ti(O*i*Pr)$_4$ (10 mol %) with 4Å molecular sieves in toluene solution were pre-activated at 110 °C for 1 h. Then benzaldehyde and Danishefsky's diene were added and reaction was processed under 0 °C for 24 h.
[b] All yields are isolated yields.
[c] Absolute configurations were *R*, which determined in all cases ee was determined by HPLC using a chiral column (Chiracel OD-H).

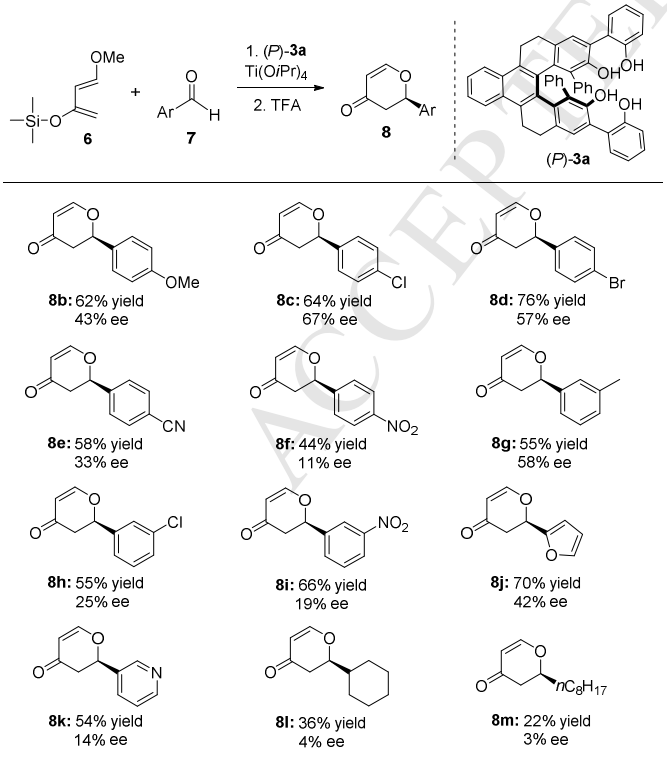

Scheme 3. The catalytic asymmetric HDA reactions of substituted aldehydes **7** with Danishefsky's diene **6**.

3. Conclusions

In conclusion, a series of optically active helicenoidal tetraols (*P*)- and (*M*)-**3a-c** with flexible tetrahydro[5]helicene core and enantiomers (*P*)- and (*M*)-**3d** with rigid [5]helicene core were conveniently synthesized by the post-functionalized strategy. Compared with **3a-c**, the [5]helicene derivative **3d** not only exhibited longer absorption and emission wavelengths, but also showed one order of magnitude amplification of the dissymmetry factor g_{lum} due to its rigid skeleton. However, it was found that enantiopure **3a-c** with more flexible skeleton were more effective in the catalytic asymmetric HDA reactions than **3d** with rigid skeleton, and under the optimal conditions, **3a-c**/Ti(O*i*Pr)$_4$ could catalyze the asymmetric HDA reactions of aromatic aldehydes and Danishefsky's diene in up to 79% yields and up to 65% ee. The results presented in this paper indicated the rigid helical structure contributed to amplifying CPL, while flexibility was beneficial to the asymmetric catalysis reaction, which could render a strategy to design and optimize the helical rigid-flexible structures to achieve amplified CPL properties and better catalytic activities.

4. Experimental section

4.1. General methods

All the reagents and solvents were commercially available and used without further purification. Reactions were carried out under inert and anhydrous conditions unless otherwise noted. ^{1}H, ^{13}C NMR spectra were recorded on Bruker® Avance 400MHz and Brucker® AVIII 500 MHz NMR spectrometers in $CDCl_3$ solutions at 298 K and the chemical shifts were reported relative to internal standard TMS (0 ppm). The UV-vis spectra were recorded on PerkinElmer® UV/vis/NIR spectrometer (Lambda 950), and the fluorescence spectra were recorded on HITACHI® F-7000 Fluorescence Spectrometer at room temperature in DCM, using 10mm cells and concentrations of 1×10^{-5} M. Absolute fluorescence quantum yield, measured by Edinburgh instruments (FLS980). CD spectra were recorded on a JASCO *J810* spectropolarimeter at room temperature in DCM. During the measurement, the instrument was thoroughly purged with nitrogen. CPL spectra were performed with a JASCO CPL-200 spectrometer at room temperature. The optical rotation was determined by Rudolph Autopol VI Automatic polarimeter. All the melting points were not calibrated and determined on YuHua X-5 digital melting point apparatus. High resolution mass spectra were obtained on the Thermo Fisher® Exactive high-resolution LC-MS spectrometer. HPLC analysis were performed on Agilent 1260 Infinity. Analytical injections were performed on chiral stationary phase using the column (Chiralpak® OD 5 μm, 4.6 mm × 250 mm, Chiralpak® IF 5 μm, 4.6 mm × 250 mm). The starting material (*P*)-**4** and (*M*)-**4** was synthesized by reported method [3].

*4.2. General procedure for the synthesis of enantiomers **3a-c** by Suzuki-Miyaura cross coupling reactions*

To the mixture of Br-H[5]HOL (*P*)-**4** or (*M*)-**4** (67 mg, 0.1 mmol), aryl boronic acid (0.5 mmol), and K_2CO_3 (138 mg, 1.0 mmol) in a mixture solution of toluene (15 mL), EtOH (15 mL), and degassed water (7.5 mL) was added $Pd(PPh_3)_2Cl_2$ (0.01 mmol). The reaction mixture was refluxed for 12 h, cooled to room temperature, and then added EA (30 mL) and water (30 mL). The organic phase was separated, dried over $MgSO_4$, and concentrated by reduced pressure. The crude product was purified by flash column chromatography.

*4.2.1. Compound (P)-**3a.*** DCM: EtOAc (*v/v* =100:1). Yellow powder (48 mg, 69% yield). $[\alpha]_D^{25}$ = –528° (*c* = 1.0 mg mL^{-1}, DCM). R_f = 0.38 (DCM: EtOAc, *v/v* =100:1). M. p.: 67-69 °C. ^{1}H NMR (500 MHz, $CDCl_3$): δ 8.18 (dd, *J* = 6.8, 3.5 Hz, 2H), 7.57 (dd, *J* = 6.7, 3.3 Hz, 2H), 7.45 (d, *J* = 9.2 Hz, 2H), 7.35 (t, *J* = 7.8 Hz, 2H), 7.28–7.20 (m, 4H), 7.13 (t, *J* = 8.4 Hz, 2H), 7.08 (d, *J* = 8.9 Hz, 2H), 7.02 (s, 2H), 6.99 (t, *J* = 7.6 Hz, 2H), 6.74 (d, *J* = 7.9 Hz, 2H), 6.36 (s, 2H), 6.24 (d, *J* = 8.4 Hz, 2H), 5.76 (s, 2H), 3.40 (d, *J* = 19.4 Hz, 2H), 2.51 (t, *J* = 17.6 Hz, 2H), 2.40 (d, *J* = 18.2 Hz, 2H), 1.57 (t, *J* = 17.2 Hz, 2H). ^{13}C NMR (126 MHz, $CDCl_3$): δ 153.8, 147.1, 135.9, 135. 8, 135.2, 131.9, 131.2, 131.1, 130.9, 130.5, 130.2, 129.4, 129.2, 129.1, 127.6, 127.4, 126.4, 126.1, 125.8, 124.5, 123.0, 121.2, 117.8, 29.3, 24.9. HRMS (APCI): calcd. for $C_{50}H_{35}O_4$ $[M-H]^-$: 699.2541, found: 699.2538.

*4.2.2. Compound (M)-**3a.*** DCM: EtOAc (*v/v* =100:1). Yellow powder (45 mg, 65% yield). $[\alpha]_D^{25}$ = +532° (*c* = 1.0 mg mL^{-1}, DCM). R_f = 0.38 (DCM: EtOAc, *v/v* =100:1). M. p.: 68-69 °C. ^{1}H NMR (500 MHz, $CDCl_3$): δ 8.18 (dd, *J* = 6.8, 3.5 Hz, 2H), 7.57 (dd, *J* = 6.7, 3.0 Hz, 2H), 7.45 (d, *J* = 8.0 Hz, 2H), 7.36 (t, *J* = 8.1 Hz, 2H), 7.27–7.20 (m, 4H), 7.13 (t, *J* = 7.7 Hz, 2H), 7.08 (d, *J* = 8.4 Hz, 2H), 7.02 (s, 2H), 6.99 (t, *J* = 7.8 Hz, 2H), 6.74 (d, *J* = 8.0 Hz, 2H), 6.36 (s, 2H), 6.24 (d, *J* = 8.5 Hz, 2H), 5.76 (s, 2H), 3.40 (d, *J* = 18.8 Hz, 2H), 2.49 (d, *J* = 15.5 Hz, 2H), 2.40 (d, *J* = 14.9 Hz, 2H), 1.57 (t, *J* = 15.0 Hz, 2H). ^{13}C NMR (126 MHz, $CDCl_3$): δ 153.8, 147.1, 135.9, 135.8, 135.2, 131.9, 131.2, 131.1, 130.9, 130.5, 130.2, 129.4, 129.2, 129.1, 127.6, 127.4, 126.4, 126.1, 125.9, 124.5, 123.0, 121.2, 117.8, 29.3, 24.9. HRMS (APCI): calcd. for $C_{50}H_{35}O_4$ $[M-H]^-$: 699.2541, found: 699.2542.

*4.2.3. Compound (P)-**3b.*** DCM as eluent. Yellow powder (52 mg, 72% yield). $[\alpha]_D^{25}$ = –536° (*c* = 1.0 mg mL^{-1}, DCM). R_f = 0.43 (DCM). M. p.: 70-72 °C. ^{1}H NMR (500 MHz, $CDCl_3$): δ 8.14 (dd, *J* = 6.3, 3.3 Hz, 2H), 7.53 (dd, *J* = 6.3, 2.9 Hz, 2H), 7.25–7.15 (m, 6H), 7.12 (d, *J* = 8.2 Hz, 2H), 6.98–6.91 (m, 6H), 6.72 (d, *J* = 7.3 Hz, 2H), 6.19 (d, *J* = 7.6 Hz, 2H), 5.71 (s, 2H), 3.36 (d, *J* = 13.9 Hz, 2H), 2.53–2.38 (m, 10H), 1.54 (t, *J* = 12.6 Hz, 2H). ^{13}C NMR (101 MHz, $CDCl_3$): δ 151.5, 147.2, 135.9, 135.2, 131.9, 131.4, 131.0, 130.5, 130.4, 123.0, 129.1, 129.0, 127.8, 127.2, 126.4, 125.8, 125.7, 124.5, 123.1, 117.6, 7, 29.3, 25.0, 20.7. HRMS (APCI): calcd. for $C_{52}H_{39}O_4$ $[M-H]^-$: 727.2854, found: 727.2855.

*4.2.4. Compound (M)-**3b.*** DCM as eluent. Yellow powder (54 mg, 74% yield). $[\alpha]_D^{25}$ = +568° (*c* = 1.0 mg mL^{-1}, DCM). R_f = 0.43 (DCM). M. p.: 70-72 °C. ^{1}H NMR (500 MHz, $CDCl_3$): δ 8.17 (dd, *J* = 6.4, 3.3 Hz, 2H), 7.55 (dd, *J* = 6.5, 3.1 Hz, 2H), 7.23–7.17 (m, 6H), 7.14 (d, *J* = 8.1 Hz, 2H), 7.00–6.94 (d, *J* = 9.7 Hz, 6H), 6.75 (d, *J* = 7.2 Hz, 2H), 6.22 (d, *J* = 7.6 Hz, 2H), 5.74 (s, 2H), 3.39 (d, *J* = 15.3 Hz, 2H), 2.53–2.38 (m, 10H), 1.56 (t, *J* = 16.5 Hz, 2H). ^{13}C NMR (101 MHz, $CDCl_3$): δ 151.5, 147.2, 135.9, 135.2, 131.9, 131.4, 131.0, 130.5, 130.4, 123.0, 129.1, 129.0, 127.8, 127.3, 126.4, 125.8, 125.7, 124.5, 123.10 117.6, 29.3, 25.0, 20.7. HRMS (APCI): calcd. for $C_{52}H_{39}O_4$ $[M-H]^-$: 727.2854, found: 727.2855.

*4.2.5. Compound (P)-**3c.*** DCM: EtOAc (*v/v* =100:1) as eluent. Yellow powder (44 mg, 60% yield). $[\alpha]_D^{25}$ = –527° (*c* = 1.0 mg mL^{-1}, DCM). R_f = 0.45 (DCM: EtOAc, *v/v* =100:1). M. p.: 73-75 °C. ^{1}H NMR (500 MHz, $CDCl_3$): δ 8.16 (dd, *J* = 6.4, 3.3 Hz, 2H), 7.56 (dd, *J* = 6.5, 3.2 Hz, 2H), 7.26–7.20 (m, *J* = 7.3, 5.9 Hz, 4H), 7.13 (dd, *J* = 9.2, 2.7 Hz, 2H), 7.03–6.99 (m, 8H), 6.66 (d, *J* = 6.6 Hz, 2H), 6.22 (d, *J* = 7.8 Hz, 2H), 5.84 (s, 2H), 3.39 (d, *J* = 17.6 Hz, 2H), 2.65–2.33 (m, 4H), 1.54 (t, *J* = 14.7 Hz, 2H). ^{13}C NMR (126 MHz, $CDCl_3$): δ 157.3 (*d*, $^1J_{C\text{-}F}$ = 238.14 Hz), 149.9, 146.8, 136.1, 135.5 (*d*, $^3J_{C\text{-}F}$ = 5.04 Hz), 132.0, 130.6 (*d*, $^3J_{C\text{-}F}$ = 5.04 Hz), 130.2, 129.5, 129.3, 127.7, 127.6, 127.2, 126.4, 126.0, 124.5, 122.4, 119.2, 119.1, 116.9 (*d*, $^2J_{C\text{-}F}$ = 22.68 Hz), 115.6 (*d*, $^2J_{C\text{-}F}$ = 22.68 Hz), 29.3, 24.9. ^{19}F NMR (377 MHz, $CDCl_3$): δ -123.79. HRMS (APCI): calcd. for $C_{52}H_{33}F_2O_4$ $[M-H]^-$: 735.2352, found: 735.2353.

*4.2.6. Compound (M)-**3c.*** DCM: EtOAc (*v/v* =100:1) as eluent. Yellow powder (46 mg, 62% yield). $[\alpha]_D^{25}$ = +515° (*c* = 1.0 mg mL^{-1}, DCM). R_f = 0.45 (DCM: EtOAc, *v/v* =100:1). M. p.: 72-74 °C. ^{1}H NMR (500 MHz, $CDCl_3$): δ 8.16 (dd, *J* = 6.4, 3.3 Hz, 2H), 7.56 (dd, *J* = 6.5, 3.2 Hz, 2H), 7.26–7.20 (m, 4H), 7.13 (dd, *J* = 9.2, 2.5 Hz, 2H), 7.07–6.97 (m, 8H), 6.66 (d, *J* = 6.6 Hz, 2H), 6.22 (d, *J* = 7.7 Hz, 2H), 5.83 (s, 2H), 3.39 (d, *J* = 13.2 Hz, 2H), 2.61–2.34 (m, 4H), 1.54 (t, *J* = 12.3 Hz, 2H). ^{13}C NMR (126 MHz, $CDCl_3$): δ 157.3 (*d*, $^1J_{C\text{-}F}$ = 239.40 Hz), 149.9, 146.8, 136.1, 135.5 (*d*, $^3J_{C\text{-}F}$ = 5.04 Hz), 132.0, 130.5 (*d*, $^3J_{C\text{-}F}$ = 5.04 Hz), 130.2, 129.5, 129.3, 127.7, 127.6, 127.2, 126.3, 126.0, 124.5, 122.4, 119.2, 119.1, 116.9 (*d*, $^2J_{C\text{-}F}$ = 22.68 Hz), 115.6 (*d*, $^2J_{C\text{-}F}$ = 22.68 Hz), 29.3, 24.9. ^{19}F NMR (377 MHz, $CDCl_3$): δ -123.79. HRMS (APCI): calcd. for $C_{52}H_{33}F_2O_4$ $[M-H]^-$: 735.2352, found: 735.2351.

*4.3. Synthesis of enantiomers **3d**.*

*4.3.1. Compound (P)-**3d***. To the solution of (*P*)-**5** (304 mg, 0.4 mmol) in xylene (100 mL) was added 2,3-dichloro-5,6-dicyanobenzoquinone (908 mg, 4 mmol) in one portion. The reaction mixture was refluxed with stirring overnight, cooled to room temperature, and concentrated by reduced pressure. Crude product was purified by flash column chromatography with DCM and petroleum ether (1:1, *v/v*) as eluent to give product. To the mixture of above product, boronic acid (276 mg, 2 mmol), and K_2CO_3 (138 mg, 4 mmol) in a mixture solution of toluene (60 mL), EtOH (60 mL), and degassed water (30 mL) was added $Pd(PPh_3)_2Cl_2$ (0.04 mmol). The reaction mixture was refluxed for 12 h, cooled to room temperature, and then added EtOAc (100 mL) and water (100 mL). The organic phase was separated, dried over $MgSO_4$, and concentrated by reduced pressure. The crude product was purified by flash column chromatography. To the solution of the above product in MeOH (20 mL) and THF (20 mL) was added Amberlyst 15 resin (400 mg). After the mixture was stirred at 65 °C overnight, the resin was filtered off, and the solvent was removed by reduced pressure. The organic layer was passed through a silica plug with DCM as eluent to afford the product (108 mg, 39% yield for three steps) as a yellow powder. $[\alpha]_D^{25}$ = +1025° (*c* = 1.0 mg mL^{-1}, DCM). R_f = 0.45 (DCM). M. p.: 73-75°C. ^{1}H NMR (500 MHz, $CDCl_3$): δ 8.68 (dd, *J* = 5.8, 3.1 Hz, 2H), 8.34 (d, *J* = 8.5 Hz, 2H), 7.74 (dd, *J* = 6.7, 2.5 Hz, 2H), 7.61 (s, 2H), 7.53–7.47 (m, 4H), 7.39 (t, *J* = 8.8 Hz, 2H), 7.19–7.04 (m, 6H), 6.92 (t, *J* = 8.2 Hz, 2H), 6.58 (t, *J* = 7.7 Hz, 2H), 6.20 (s, 2H), 6.13 (s, 2H), 5.64 (d, *J* = 7.8 Hz, 2H). ^{13}C NMR (126 MHz, $CDCl_3$): δ 153.9, 148.1, 135.5, 132.3, 131.3, 130.2, 129.9, 129.7, 129.0, 128.9, 128.8, 128.5, 128.1, 127.9, 127.2, 126.3, 125.9, 125.6, 125.1, 124.9, 123.6, 121.3, 117.6, 117.4. HRMS (APCI): calcd. for $C_{52}H_{39}O_4$ $[M-H]^-$: 695.2228, found: 695.2223.

*4.3.2. Compound (M)-**3d.*** According to the same method as the preparation of (*P*)-**3d**, compound (*M*)-**3d** was obtained. DCM as eluent. Yellow powder (88 mg, 32% yield). $[\alpha]_D^{25}$ = –1032° (*c* = 1.0 mg mL^{-1}, DCM). R_f = 0.45 (DCM). M. p.: 74-76 °C. ^{1}H NMR (500 MHz, $CDCl_3$): δ 8.68 (dd, *J* = 7.8, 4.7 Hz, 2H), 8.33 (d, *J* = 8.7 Hz, 2H), 7.73 (dd, *J* = 6.2, 3.1 Hz, 2H), 7.61 (s, 2H), 7.57–7.45 (m, 4H), 7.38 (t, *J* = 8.8 Hz, 2H), 7.18–7.03 (m, 6H), 6.93 (t, *J* = 8.3 Hz, 2H), 6.58 (t, *J* = 9.0 Hz, 2H), 6.20 (s, 2H), 6.13 (s, 2H), 5.64 (d, *J* = 8.2 Hz, 2H). ^{13}C NMR (126 MHz, $CDCl_3$): δ 153.9, 148.1, 135.5, 132.3, 131.3, 130.2, 129.9, 129.7, 129.0, 128.9, 128.8, 128.5, 128.1, 127.9, 127.2, 126.3, 125.9, 125.6, 125.1, 124.9, 123.6, 121.3, 117.7, 117.4. HRMS (APCI): calcd. for $C_{52}H_{39}O_4$ $[M-H]^-$: 695.2228, found: 695.2228.

4.4. General catalytic asymmetric HDA procedure.

A mixture of PhOH-H[5]HOL (35.0 mg, 0.05 mmol), 1.0 M $Ti(OiPr)_4$ in CH_2Cl_2 (100 µL, 0.10 mmol), and activated 4 Å molecular sieves (240 mg) in toluene (5 mL) was heated at 110 °C for 1 h. The yellow mixture was cooled to rt, and arylaldehyde (0.5 mmol) was added. The mixture was stirred for 10 min and cooled to 0 °C. Danishefsky's diene (120 µL, 0.60 mmol) was added. The mixture was allowed to stir at 0 °C for 24 h, and then treated with 5 drops of trifluoroacetic acid (TFA). After the mixture was stirred at 0 °C for 15 min, saturated $NaHCO_3$ (5.0 mL) was added. The mixture was stirred for 10 min, and then filtered through a plug of Celite. The organic layer was separated, and the aqueous layer was extracted with ether (5 × 3 mL). The combined organic layer was dried over anhydrous $MgSO_4$ and concentrated. The crude residue was purified by flash chromatography (EtOAc: petroleum ether = 1:4, R_f = 0.52) to yield product.

*4.4.1. Compound (R)-**8a**.* Colorless oil (69 mg, 79% yield); Enantiomeric excess: 53%; ^{1}H NMR (500 MHz, $CDCl_3$): δ 7.28 (d, *J* = 6.0 Hz, 1H), 7.25–7.16 (m, 5H), 5.33 (d, *J* = 6.0 Hz, 1H), 5.23 (d, *J* = 14.4 Hz, 1H), 2.78–2.59 (m, 1H), 2.46 (dd, *J* = 18.5, 2.6 Hz, 1H). ^{13}C NMR (126 MHz, $CDCl_3$): δ 191.1, 162.2, 136.8, 127.9, 125.1, 106.3, 80.1, 76.3, 76.1, 75.8, 42.4. HPLC analysis: Daicel Chiralpak OD-H, Hexane/IPA = 99:1, flow rate = 1.0 mL/min, retention time: 24.60 min (minor) and 29.33 min (major).

*4.4.2. Compound (R)-**8b**.* White solid (63 mg, 62% yield); Enantiomeric excess: 43%; M. p.: 51-53 °C; [lit. [58] M. p.: 50-51 °C]; ^{1}H NMR (500 MHz, $CDCl_3$): δ 7.40 (d, *J* = 6.0 Hz, 1H), 7.28 (d, *J* = 8.6 Hz, 2H), 6.89 (d, *J* = 8.7 Hz, 2H), 5.45 (d, *J* = 6.0 Hz, 1H), 5.31 (dd, *J* = 14.4, 3.2 Hz, 1H), 3.76 (s, 3H), 2.86 (dd, *J* = 16.8, 14.5 Hz, 1H), 2.56 (dd, *J* = 16.8, 2.5 Hz, 1H). ^{13}C NMR (126 MHz, $CDCl_3$): δ 192.3, 163.3, 160.0, 129.9, 127.8, 114.1, 107.2, 80.8, 55.3, 43.1. HPLC analysis: Daicel Chiralpak OD-H, Hexane/IPA = 90:10, flow rate = 1.0 mL/min, retention time: 14.30 min (minor) and 15.52 min (major).

*4.4.3. Compound (R)-**8c**.* White solid (67 mg, 64% yield); Enantiomeric excess: 67%; M. p.: 70-71 °C; [lit. [58] M. p.: 69-71 °C]; ^{1}H NMR (500 MHz, $CDCl_3$): δ 7.47 (d, *J* = 6.0 Hz, 1H), 7.40 (d, *J* = 6.9 Hz, 2H), 7.34 (d, *J* = 8.2 Hz, 2H), 5.53 (d, *J* = 6.0 Hz, 1H), 5.41 (d, *J* = 14.3 Hz, 1H), 2.86 (dd, *J* = 16.6, 14.5 Hz, 1H), 2.65 (d, *J* = 19.8 Hz, 1H). ^{13}C NMR (126 MHz, $CDCl_3$) δ 191.6, 162.9, 136.4, 134.8, 129.1, 127.5, 107.5, 80.3, 43.3. HPLC analysis: Daicel Chiralpak OD-H, Hexane/IPA = 90:10, flow rate = 1.0 mL/min, retention time: 23.34 min (minor) and 30.43 min (major).

*4.4.4. Compound (R)-**8d**.* Colorless oil (95 mg, 76% yield); Enantiomeric excess: 57%; ^{1}H NMR (500 MHz, $CDCl_3$): δ 7.55 (d, *J* = 8.4 Hz, 2H), 7.47 (d, *J* = 6.0 Hz, 1H), 7.28 (d, *J* = 8.4 Hz, 2H), 5.53 (d, *J* = 6.0 Hz, 1H), 5.39 (dd, *J* = 14.3, 3.3 Hz, 1H), 2.85 (dd, *J* = 16.8, 14.4 Hz, 1H).^{13}C NMR (126 MHz, $CDCl_3$): δ 191.6, 162.9, 136.9, 132.0, 127.7, 122.9, 107.5, 80.3, 43.3. HPLC analysis: Daicel Chiralpak OD-H, Hexane/IPA = 90:10, flow rate = 1.0 mL/min, retention time: 11.36 min (minor) and 14.15 min (major).

*4.4.5. Compound (R)-**8e**.* White solid (58 mg, 58% yield); Yield: 59%; M. p.: 72-73 °C; [lit. [58] M. p.: 70-72 °C]; Enantiomeric excess: 33%. ^{1}H NMR (500 MHz, $CDCl_3$): δ 7.75 (d, *J* = 8.2 Hz, 2H), 7.53 (dd, *J* = 16.4, 7.1 Hz, 3H), 5.58 (d, *J* = 6.0 Hz, 1H), 5.52 (dd, *J* = 14.1, 3.5 Hz, 1H), 2.84 (dd, *J* = 16.7, 14.2 Hz, 1H), 2.72 (dd, *J* = 16.8, 3.2 Hz, 1H). ^{13}C NMR (126 MHz, $CDCl_3$): δ 190.8, 162.6, 143.0, 132.7, 126.5, 118.3, 112.8, 107.8, 79.9, 43.3. HPLC analysis: Daicel Chiralpak OD-H, Hexane/IPA = 90:10, flow rate = 1.0 mL/min, retention time: 27.28 min (minor) and 32.49 min (major).

*4.4.6. Compound (R)-**8f**.* White solid (48 mg, 44% yield); Yield: 43%; M. p.: 101-102 °C; [lit. [58] M. p.: 100-102 °C]; Enantiomeric excess: 11%. ^{1}H NMR (500 MHz, $CDCl_3$): δ 8.30 (d, *J* = 8.6 Hz, 2H), 7.60 (d, *J* = 8.6 Hz, 2H), 7.52 (d, *J* = 6.0 Hz, 1H), 5.62 – 5.51 (m, 2H), 2.85 (dd, *J* = 16.7, 14.2 Hz, 1H), 2.75 (d, *J* = 3.6 Hz, 1H). ^{13}C NMR (126 MHz, $CDCl_3$): δ 190.7, 162.5, 148.1, 144.9, 126.7, 124.2, 107.9, 43.4. HPLC analysis: Daicel Chiralpak OD-H, Hexane/IPA = 90:10, flow rate = 1.0 mL/min, retention time: 29.36 min (minor) and 40.16 min (major).

*4.4.7. Compound (R)-**8g**.* Colorless oil (52 mg, 55% yield); Enantiomeric excess: 58%. ^{1}H NMR (500 MHz, $CDCl_3$): δ 7.45 (d, *J* = 6.0 Hz, 1H), 7.34–7.23 (m, 1H), 7.23–7.11 (m, 3H), 5.54–5.43 (m, 1H), 5.37 (dd, *J* = 14.5, 3.2 Hz, 1H), 2.89 (dd, *J* = 16.8, 14.6 Hz, 1H), 2.63 (d, *J* = 19.5 Hz, 1H), 2.38 (s, 3H). ^{13}C NMR (126 MHz, $CDCl_3$): δ 192.1, 163.2, 138.6, 137.8, 129.7, 128.7, 126.8, 123.2, 107.3, 81.2, 43.4, 21.4. HPLC analysis: Daicel Chiralpak OD-H, Hexane/IPA = 90:10, flow rate = 1.0 mL/min, retention time: 8.83 min (minor) and 10.05 min (major).

*4.4.8. Compound (R)-**8h**.* White solid (57 mg, 55% yield); M. p.: 73-74 °C; [lit. [57] M. p.: 74-75 °C]; Enantiomeric excess: 25%. ^{1}H NMR (500 MHz, $CDCl_3$): δ 7.57 (d, *J* = 7.7 Hz, 1H), 7.50 (d, *J* = 6.0 Hz, 1H), 7.42–7.23 (m, 3H), 5.79 (dd, *J* = 13.9, 3.9 Hz, 1H), 5.53 (d, *J* = 6.0 Hz, 1H), 2.84–2.58 (m, 2H). ^{13}C NMR (126 MHz, $CDCl_3$): δ 191.3, 163.0, 135.8, 131.5, 129.7, 129.7, 127.4, 127.1, 107.5, 77.9, 42.1. HPLC analysis: Daicel Chiralpak OD-H, Hexane/IPA = 90:10, flow rate = 1.0 mL/min, retention time: 15.13 min (minor) and 16.63 min (major).

*4.4.9. Compound (R)-**8i**.* Colorless oil (73 mg, 66% yield); Yield: 67%; Enantiomeric excess: 19%. ^{1}H NMR (500 MHz, $CDCl_3$): δ 8.05 (d, *J* = 8.2 Hz, 1H), 7.86 (d, *J* = 7.8 Hz, 1H), 7.76 (t, *J* = 7.6 Hz, 1H), 7.57 (t, *J* = 7.8 Hz, 1H), 7.50 (d, *J* = 6.1 Hz, 1H), 6.06 (dd, *J* = 14.1, 3.1 Hz, 1H), 5.58 (d, *J* = 6.0 Hz, 1H), 2.99–2.96 (m, 1H), 2.84–2.69 (m, 1H). ^{13}C NMR (126 MHz, $CDCl_3$): δ 190.8, 162.6, 147.2, 133.8, 129.5, 128.1, 124.9, 107.9, 43.1. HPLC analysis: Daicel Chiralpak OD-H, Hexane/IPA = 90:10, flow rate = 1.0 mL/min, retention time: 16.81 min (minor) and 20.20 min (major).

*4.4.10. Compound (R)-**8j**.* White solid (58 mg, 70% yield); M. p.: 70-71 °C; [lit. [58] M. p.: 72-73 °C]; Enantiomeric excess: 42%. ^{1}H NMR (500 MHz, $CDCl_3$): δ 7.48–7.47 (m, 1H), 7.36 (d, *J* = 6.1 Hz, 1H), 6.45 (d, *J* = 3.3 Hz, 1H), 6.40 (d, *J* = 1.7 Hz, 1H), 5.49–5.45 (m, 2H), 3.06 (dd, *J* = 16.9, 12.8 Hz, 1H), 2.73–2.69 (m, 1H). ^{13}C NMR (126 MHz, $CDCl_3$): δ 191.1, 162.4, 150.1, 143. 6, 110.1, 109. 7, 107.3, 73.5, 39.5. HPLC analysis: Daicel Chiralpak OD-H, Hexane/IPA = 90:10, flow rate = 1.0 mL/min, retention time: 21.99 min (major) and 24.18 min (minor).

*4.4.11. Compound (R)-**8k**.* White solid (47 mg, 54% yield); M. p.: 73-75 °C; [lit. [57] M. p.: 73-74 °C]; Enantiomeric excess: 14%. ^{1}H NMR (500 MHz, $CDCl_3$): δ 8.69–8.57 (m, 1H), 7.79 (t, *J* = 7.7 Hz, 1H), 7.55–7.43 (m, 2H), 7.34–7.27 (m, 1H), 5.63–5.46 (m, 2H), 3.07–2.94 (m, 1H), 2.92–2.78 (m, 1H). ^{13}C NMR (126 MHz, $CDCl_3$): δ 191.8, 162.4, 156.7, 149.5, 137.2, 123.6, 120.9, 107.8, 81.1, 41.6. HPLC analysis: Daicel Chiralpak OD-H, Hexane/IPA = 90:10, flow rate = 1.0 mL/min, retention time: 27.78 min (major) and 34.99 min (minor).

*4.4.12. Compound (R)-**8l**.* Colorless oil (32 mg, 36% yield); Enantiomeric excess: 4%. ^{1}H NMR (500 MHz, $CDCl_3$): δ 7.38

(d, *J* = 6.0 Hz 1H), 5.38 (d, *J* = 6.0 Hz 1H), 4.25–4.07 (m, 1H), 2.62–2.47 (m, 1H), 2.38 (d, *J* = 16.6 Hz, 1H), 1.96–1.86 (m, 1H), 1.80 (d, *J* = 12.8 Hz, 2H), 1.68 (d, *J* = 11.0 Hz, 2H), 1.34–1.00 (m, 6H). ^{13}C NMR (126 MHz, $CDCl_3$): δ 193.2, 163.3, 106.8, 83.6, 77.4, 77.1, 76.9, 41.4, 39.1, 28.0, 26.1, 25.8. HPLC analysis: Daicel Chiralpak OD-H, Hexane/IPA = 90:10, flow rate = 1.0 mL/min, retention time: 9.87 min (major) and 10.99 min (minor).

*4.4.13. Compound (R)-**8m.*** Colorless oil (23 mg, 22% yield); Enantiomeric excess: 3%. ^{1}H NMR (500 MHz, $CDCl_3$): δ 7.36 (d, *J* = 5.9 Hz, 1H), 5.40 (dd, *J* = 6.0, 1.1 Hz, 1H), 4.45–4.35 (m, 1H), 2.52 (dd, *J* = 16.8, 13.4 Hz, 1H), 2.43 (dd, *J* = 16.8, 3.8, 1H), 1.85–1.81 (m, 1H), 1.69–1.62 (m, 1H), 1.49–1.25 (m, 12H), 0.89 (t, *J* = 6.8 Hz, 3H). ^{13}C NMR (126 MHz, $CDCl_3$): δ 192.8, 163.3, 106.9, 79.6, 77.4, 77.1, 76.9, 41.9, 34.4, 31.8, 29.4, 29.3, 24.8, 22.7, 14.1. HPLC analysis: Daicel Chiralpak OD-H, Hexane/IPA = 90:10, flow rate = 1.0 mL/min, retention time: 17.21 min (minor) and 18.60 min (major).

Acknowledgement

We thank the National Natural Science Foundation of China (21572233, 21332008), the National Basic Research Program (2015CB856502), and the Strategic Priority Research Program of Chinese Academy of Sciences (XDB12010400) for financial supports.

Conflicts of interest

There are no conflicts to declare.

Appendix A. Supplementary data

Supplementary data associated with this article can be found, in the online version, at https://doi.org/10.1016

References

1. Y. Shen and C.-F. Chen, Chem. Rev. 112 (2012) 1463-1535.
2. M. Li, X.-J. Li, H.-Y. Lu and C.-F. Chen, Sens. Actuat. B 202 (2014) 583-587.
3. L. Fang, M. Li, W.-B. Lin, Y. Shen and C.-F. Chen, J. Org. Chem. 82 (2017) 7402-7409.
4. D. Schweinfurth, M. Zalibera, M. Kathan, C. Shen, M. Mazzolini, N. Trapp, J. Crassous, G. Gescheidt and F. Diederich, J. Am. Chem. Soc. 136 (2014) 13045-13052.
5. M. Li, W. Yao, J.-D. Chen, H.-Y. Lu, Y. Zhao and C.-F. Chen, J. Mater. Chem. C 2 (2014) 8373-8380.
6. M. Li, Y. Niu, H.-Y. Lu and C.-F. Chen, Dye Pigment 120 (2015) 184-189.
7. D. Yang, M. Li and C. Chen, Chin. J. Chem. 35 (2017) 635-639.
8. Y. Mou, H. Lu, M. Li and C. Chen, Chin. J. Chem. 35 (2017) 435-441.
9. M. Gingras, G. Felix and R. Peresutti, Chem. Soc. Rev. 42 (2013) 1007-1050.
10. L. Fang, W. Lin, Y. Shen and C. Chen, Chin. J. Org. Chem. 38 (2018) 541-554.
11. W.-B. Lin, M. Li, L. Fang and C.-F. Chen, Chin. Chem. Lett. 2018, **29**, 40.
12. K. Nakamura, S. Furumi, M. Takeuchi, T. Shibuya and K. Tanaka, J. Am. Chem. Soc. 136 (2014) 5555-5558.
13. Y. Sawada, S. Furumi, A. Takai, M. Takeuchi, K. Noguchi and K. Tanaka, J. Am. Chem. Soc. 134 (2012) 4080-4083.
14. D.-Q. He, H.-Y. Lu, M. Li and C.-F. Chen, Chem. Commun 53 (2017) 6093-6096.
15. H. Oyama, K. Nakano, T. Harada, R. Kuroda, M. Naito, K. Nobusawa and K. Nozaki, Org. Lett. 15 (2013) 2104-2107.
16. T. Kaseyama, S. Furumi, X. Zhang, K. Tanaka and M. Takeuchi, Angew. Chem. Int. Ed. 50 (2011) 3684-3687.
17. T. Fujikawa, Y. Segawa and K. Itami, J. Am. Chem. Soc. 137 (2015) 7763-7768.
18. Y. Yamamoto, H. Sakai, J. Yuasa, Y. Araki, T. Wada, T. Sakanoue, T. Takenobu, T. Kawai and T. Hasobe, Chem. Eur. J. 22 (2016) 4263-4273.
19. M. Li, W.-B. Lin, L. Fang and C.-F. Chen, Acta Chim. Sinica 75 (2017) 1150-1163.
20. D. Yang, P. Duan, L. Zhang and M. Liu, Nat. Commun. 8 (2017) 15727.
21. H. Tsumatori, T. Nakashima and T. Kawai, Org. Lett. 12 (2010) 2362-2365.
22. J. Han, P. Duan, X. Li and M. Liu, J. Am. Chem. Soc. 139 (2017) 9783-9786.
23. J. Kumar, H. Tsumatori, J. Yuasa, T. Kawai and T. Nakashima, Angew. Chem. Int. Ed. 54 (2015) 5943-5947.
24. J. Kumar, T. Nakashima, H. Tsumatori and T. Kawai, J Phys. Chem. Lett. 5 (2014) 316-321.
25. M. T. Reetz, E. W. Beuttenmuller and R. Goddard, Tetrahedron Lett. 38 (1997) 3211-3214.
26. D. Nakano and M. Yamaguchi, Tetrahedron Lett. 44 (2003) 4969-4971.
27. Z. Krausova, P. Sehnal, B. P. Bondzic, S. Chercheja, P. Eilbracht, I. G. Stara, D. Saman and I. Stary, Eur. J. Org. Chem. (2011) 3849-3857.
28. T. Tsujihara, N. Inada-Nozaki, T. Takehara, D.-Y. Zhou, T. Suzuki and T. Kawano, Eur. J. Org. Chem. (2016) 4948-4952.
29. K. Yamamoto, T. Shimizu, K. Igawa, K. Tomooka, G. Hirai, H. Suemune and K. Usui, Sci. Rep. 6 (2016) 36211.
30. P. Aillard, D. Dova, V. Magne, P. Retailleau, S. Cauteruccio, E. Licandro, A. Voituriez and A. Marinetti, Chem. Commun. 52 (2016) 10984-10987.
31. P. Aillard, P. Retailleau, A. Voituriez and A. Marinetti, Chem. Eur. J. 21 (2015) 11989-11993.
32. R. El Abed, F. Aloui, J.-P. Genet, B. Ben Hassine and A. Marinetti, J. Organomet. Chem. 692 (2007) 1156-1160.
33. F. Aloui, R. El Abed, A. Marinetti and B. Ben Hassine, Tetrahedron Lett. 48 (2007) 2017-2020.
34. P. Aillard, A. Voituriez, D. Dova, S. Cauteruccio, E. Licandro and A. Marinetti, Chem. Eur. J. 20 (2014) 12373-12376.
35. M. Gicquel, Y. Zhang, P. Aillard, P. Retailleau, A. Voituriez and A. Marinetti, Angew. Chem. Int. Ed. 54 (2015) 5470-5473.
36. K. Yavari, P. Retailleau, A. Voituriez and A. Marinetti, Chem. Eur. J. 19 (2013) 9939-9947.
37. K. Yavari, P. Aillard, Y. Zhang, F. Nuter, P. Retailleau, A. Voituriez and A. Marinetti, Angew. Chem. Int. Ed. 53 (2014) 861-865.
38. P. Aillard, A. Voituriez and A. Marinetti, Dalton Trans. 43 (2014) 15263-15278.
39. P. Aillard, P. Retailleau, A. Voituriez and A. Marinetti, Chem. Commun. 50 (2014) 2199-2201.
40. K. Yavari, S. Moussa, B. Ben Hassine, P. Retailleau, A. Voituriez and A. Marinetti, Angew. Chem. Int. Ed. 51 (2012) 6748-6752.
41. M. R. Crittall, H. S. Rzepa and D. R. Carbery, Org. Lett. 13 (2011) 1250-1253.
42. M. R. Crittall, N. W. G. Fairhurst and D. R. Carbery, Chem. Commun. 48 (2012) 11181-11183.
43. J. Misek, F. Teply, I. G. Stara, M. Tichy, D. Saman, I. Cisarova, P. Vojtisek and I. Stary, Angew. Chem. Int. Ed. 47 (2008) 3188-3191.
44. J. Chen, B. Captain and N. Takenaka, Org. Lett. 13 (2011) 1654-1657.
45. N. Takenaka, J. Chen, B. Captain, R. S. Sarangthem and A. Chandrakumar, J. Am. Chem. Soc. 132 (2010) 4536-4537.

46. N. Takenaka, R. S. Sarangthem and B. Captain, Angew. Chem. Int. Ed. 47 (2008) 9708-9710.
47. M. J. Narcis, D. J. Sprague, B. Captain and N. Takenaka, Org. Biomol. Chem. 10 (2012) 9134-9136.
48. Z. Peng, M. J. Narcis and N. Takenaka, Molecules 18 (2013) 9982-9998.
49. S. D. Dreher, T. J. Katz, K.-C. Lam and A. L. Rheingold, J. Org. Chem. 65 (2000) 815-822.
50. J.-D. Chen, L. Fang and C.-F. Chen, Mini-Rev. Org. Chem. 12 (2015) 310-327.
51. X.-Y. Yuan and Z.-P. Zhang, Chin. J. Org. Chem. 27 (2007) 1479-1490.
52. M. Li, H.-Y. Lu and C.-F. Chen, J. Photochem. Photobio. A: Chem. 355 (2018) 408-413.
53. H. Du, X. Zhang, Z. Wang, H. Bao, T. You and K. Ding, Eur. J. Org. Chem. (2008) 2248-2254.
54. B. Wang, X. Feng, X. Cui, H. Liu and Y. Jiang, Chem. Commun, 17 (2000) 1605-1606.
55. H. Du, J. Long, J. Hu, X. Li and K. Ding, Org. Lett. 4 (2002) 4349-4352.
56. X. B. Yang, J. Feng, J. Zhang, N. Wang, L. Wang, J. L. Liu and X. Q. Yu, Org. Lett. 10 (2008) 1299.
57. B. Wang, X. Feng, Y. Huang, H. Liu, X. Cui and Y. Jiang, J. Org. Chem. 67 (2002) 2175-2182.
58. M. Anada, T. Washio, N. Shimada, S. Kitagaki, M. Nakajima, M. Shiro and S. Hashimoto, Angew. Chem. Int. Ed. 43 (2004) 2665-2668.